Kinetics of Electron Self-Exchange Reactions between Metalloporphyrin Sites in Submicrometer Polymeric Films on Electrodes

B. A. White and R. W. Murray*

Contribution from the Kenan Laboratories of Chemistry, University of North Carolina, Chapel Hill, North Carolina 27514. *Received August 18, 1986*

Abstract: Electron-transfer kinetics and axial-ligation reactions are explored within films of polymeric Fe, Co, Ni, and Cu tetraphenylporphyrins on electrodes. By sandwiching 100–300-nm films between two electrodes potentiostated so as to reduce and oxidize opposing faces of the polymer film, it was possible to determine that electron mobilities within the porphyrin film vary by over $10^3\times$ depending on central metal, porphyrin oxidation state, and axial ligation. Mobilities were measured as electron diffusion coefficients, which, since electron transport occurs by a hopping process, are proportional to the electron self-exchange rate constants of each oxidation state couple. The electron diffusion coefficients in the polymeric porphyrin films are shown to parallel the heterogeneous electron-transfer rate constants that have been determined for solutions of analogous *monomeric* tetraphenylporphyrins at electrode surfaces. It is concluded that electron-transfer barriers within the polymeric porphyrins are similar to those of dissolved monomers. Such a comparison has not been previously reported for a series of related electron-transfer processes. Electron diffusion coefficients could also be measured for a Fe(III/II) porphyrin film in the absence of liquid solvent.

Metalloporphyrin electron-transfer reactions are essential components of numerous chemical, photochemical, and biological processes, including mitochondrial electron transport, dioxygen activation, and photosynthesis.[1] Studies of electron-transfer kinetics of model metalloporphyrins can contribute to a better understanding of these complex chemical or biological redox reactions. Such kinetic studies, for monomeric metalloporphyrin solutes, have been based on cyclic voltammetry,[2-6] NMR line broadening,[7] and the Marcus cross-reaction relationships,[8] but remain relatively limited in number and scope. This paper describes a new approach to measurement of metalloporphyrin electron self-exchange kinetics, by an approach based on studying electron-hopping rates in ultrathin films (100–300 nm) of metalloporphyrin polymers sandwiched between two electrodes.

The ultrathin metalloporphyrin polymer films are prepared by electrooxidative electropolymerization[9,10] of metallotetra(*o*-aminophenyl)porphyrins, M(*o*-NH_2)TPP. A porous film of Au is evaporated onto the surface of the polymeric porphyrin film so as to form a sandwich electrode,[11] the Au side of which is porous to solvent, electrolyte ions, gaseous vapors,[12] or other chosen bathing media. Currents flow between the Pt and Au electrodes when their potentials are adjusted so as to oxidize and reduce the members of a selected redox couple on opposing faces of the metalloporphyrin polymer film. The currents measure the rate of electron transport, which, by application of Fick's law, is expressed[11] as the electron diffusion coefficient, D_e. Charge transport in these and other fixed-site, localized state (redox) polymers[13] is believed to occur by electron self-exchange (electron hopping) between neighboring oxidized and reduced porphyrin sites in the films. The electron diffusion coefficient has been shown[14] to be proportional to the more familiar electron self-exchange rate constant, k_{ex}, in fixed-site redox polymers.

We have applied the electron diffusion measurement to a variety of redox couples in poly-M(*o*-NH_2)TPP films in which M = Fe, Co, Ni, and Cu and in the presence of several different axial ligands. The electron self-exchange kinetic constants thus derived for the polymeric porphyrin sites parallel those known for dissolved, monomeric metalloporphyrins. Such a relationship in a series of polymeric redox couples has not been previously established.

Experimental Section

Materials. H_2(*o*-NH_2)TPP was synthesized according to a published procedure.[15a] Metal insertions[16] were accomplished using $Ni(OAc)_2\cdot 4H_2O$ and the anhydrous chlorides of Fe(II), Co(II), and Cu(II), with complete metalation being verified by UV–visible spectroscopy. The M(*o*-NH_2)TPP products exist as statistical mixtures of four atropisomers;[15a] the mixture is used directly in electrochemical solutions. Tetraethylammonium perchlorate (Et_4NClO_4) was thrice recrystallized from water, and tetraethylammonium chloride (Et_4NCl) was thrice precipitated from CH_2Cl_2 with diethyl ether. Electrolytes were dried in a vacuum oven at 50 °C. Spectroquality acetonitrile (CH_3CN, Burdick and Jackson) was dried twice with activated 4-A molecular sieves. Reagent grade pyridine (py) was stored over activated 4-A molecular sieves. Other chemicals were reagent grade or better and were used as received.

Methods. Glass-shrouded Pt minidisk electrodes[11] (areas = 0.0032 and 0.0020 cm^2, polished with 1-μm diamond paste, Buehler) and a Model RDE3 bipotentiostat (Pine Instrument Co., Grove City, PA) were used for sandwich electrode voltammetry, and Teflon-shrouded Pt disk electrodes and a locally constructed potentiostat were used for standard cyclic voltammetry. The room-temperature solutions, in conventional three-compartment cells, were deoxygenated with Ar that had been passed through a solid oxygen-removal catalyst (Ridox), activated 4-A molecular sieves, and dry CH_3CN. A Pt wire or gauze (for electropolymerizations) served as auxiliary electrode and the reference electrode was $Ag/AgClO_4$ in 0.1 M Et_4NClO_4/CH_3CN. Potentials are reported on the NaCl-saturated SCE (SSCE) potential scale, making the scale

(1) Dolphin, D., Ed. *The Porphyrins*; Academic Press: New York, 1978.
(2) Kadish, K. M.; Davis, D. G. *Ann. N. Y. Acad. Sci.* **1973**, *206*, 495.
(3) Kadish, K. M.; Morrison, M. M.; Constant, L. A.; Dickens, L.; Davis, D. G. *J. Am. Chem. Soc.* **1976**, *98*, 8387.
(4) Chang, D.; Malinski, T.; Ulman, A.; Kadish, K. M. *Inorg. Chem.* **1984**, *23*, 817.
(5) Constant, L. A.; Davis, D. G. *J. Electroanal. Chem.* **1976**, *74*, 85.
(6) Truxillo, L. A.; Davis, D. G. *Anal. Chem.* **1975**, *47*, 2260.
(7) (a) Shirazi, A.; Barbush, M.; Ghosh, S.; Dixon, D. W. *Inorg. Chem.* **1985**, *24*, 2495. (b) Dixon, D. W.; Barbush, M.; Shirazi, A. *Ibid.* **1985**, *24*, 1081.
(8) Langley, R.; Hambright, P.; Williams, R. F. X. *Inorg. Chim. Acta* **1985**, *104*, L25 and ref 14–20 therein.
(9) (a) White, B. A.; Murray, R. W. *J. Electroanal. Chem.* **1985**, *189*, 345. (b) Bettelheim, A.; White, B. A.; Raybuck, S. A.; Murray, R. W. *Inorg. Chem.*, in press.
(10) The polymers form by aniline-like coupling reactions[9] following oxidation of the aminophenyl substituents.
(11) Pickup, P. G.; Kutner, W.; Leidner, C. R.; Murray, R. W. *J. Am. Chem. Soc.* **1984**, *106*, 1991.
(12) Jernigan, J. C.; Chidsey, C. E. D.; Murray, R. W. *J. Am. Chem. Soc.* **1985**, *107*, 2824.
(13) Kaufman, F. B.; Engler, E. M. *J. Am. Chem. Soc.* **1979**, *101*, 547.
(14) (a) Andrieux, C. P.; Saveant, J. M. *J. Electroanal. Chem.* **1980**, *111*, 377. (b) Laviron, E. *Ibid.* **1980**, *112*, 1.
(15) (a) Collman, J. P.; Gagne, R. R.; Reed, C. A.; Halbert, T. R.; Land, G.; Robinson, W. T. *J. Am. Chem. Soc.* **1975**, *97*, 1427. (b) Kadish, K. M.; Larson, G.; Lexa, D.; Momenteau, M. *Ibid.* **1975**, *97*, 282. (c) Bottomly, L. A.; Ercolani, C.; Gorce, J.-N.; Pennesi, G.; Rossi, G. *Inorg. Chem.* **1986**, *25*, 2338.
(16) Adler, A. D.; Longo, F. R.; Kampas, K.; Kim, J. *J. Inorg. Nucl. Chem.* **1970**, *32*, 2443.

0002-7863/87/1509-2576$01.50/0

Table I. Formal Potentials[a] of Metallotetra(*o*-aminophenyl)porphyrin Monomers and Their Electropolymerized Films

	$E°'$, V vs SSCE					
	0.1 M Et_4NClO_4		0.2 M Et_4NCl[c]		0.1 M Et_4NClO_4, 1 M pyridine	
reaction[b]	solution	polymer	solution	polymer	solution	polymer
$PFe^{III/II}$	−0.27	+0.17[d]	−0.30	−0.30[d]	+0.08	+0.15
$PFe^{II/I}$	−1.08	−1.05[d]	−1.21	−1.17[d]		
$(P^{0/\cdot-})Fe^{I}$	−1.67	−1.69	−1.64	−1.64		
$PCo^{II/I}$	−0.86	−0.86			−1.04	−1.06
$(P^{0/\cdot-})Cu^{II}$	−1.28	−1.27				
$(P^{0/\cdot-})Ni^{II}$	−1.28	−1.30				

[a] In CH_3CN. Electrochemical potentials were measured vs. $Ag/AgClO_4$ in 0.1 M Et_4NClO_4/CH_3CN and converted to the SSCE scale using the potential of the ferrocene/ferrocenium couple which in 0.1 M Et_4NClO_4/CH_3CN is +0.39 and +0.19 V vs. SSCE and $Ag/AgClO_4$, respectively. [b] P represents the dianion of (*o*-NH_2)TPP. [c] The junction potential between 0.2 M Et_4NCl/CH_3CN and 0.1 M Et_4NClO_4/CH_3CN, evaluated using the ferrocene/ferrocenium potential, was ≤10 mV. [d] Corrections of values given in ref 9a.

conversion using the ferrocene/ferrocenium couple potential which in 0.1 M Et_4NClO_4/CH_3CN is +0.39 and +0.19 V vs. SSCE and $Ag/AgClO_4$, respectively.

Oxidative electropolymerization[9] of poly-M(*o*-NH_2)TPP films onto electrodes was accomplished from 0.7–0.8 mM monomer solutions in 0.1 M Et_4NClO_4/CH_3CN, cycling the working electrode potential at 200 mV/s between 0.0 and +1.03 (±0.03) V. (A small portion of the monomer often did not dissolve in CH_3CN, despite ultrasonification, perhaps owing to unequal atropisomer solubilities.) In order to deposit the relatively thick films used on Pt minidisk electrodes, the following modifications were employed: (i) monomer solutions were magnetically stirred during electropolymerization, (ii) 0.8 M Et_4NClO_4 was used[17] in polymerizations of Co(*o*-NH_2)TPPCl, and (iii) the potential was held constant near +1.00 V for polymerizations of Fe(*o*-NH_2)TPPCl. The quantities of electropolymerized, electroactive porphyrin (surface coverage, Γ_T, mol/cm^2) were determined (before Au deposition) by measuring the electrochemical charge under slow potential scan cyclic voltammograms[18] in deaerated 0.1 M Et_4NClO_4/CH_3CN (for the Co, Ni, and Cu porphyrin polymers) or in deaerated 0.2 M Et_4NCl/CH_3CN (for poly-Fe(*o*-NH_2)TPPX).[18] The thicknesses, *d*, of air-dried poly-Co(*o*-NH_2)TPP films of known Γ_T grown on SnO_2 films on glass were measured by surface profilometry (Tencor/Alpha Step 100).

Sandwich electrodes were prepared[11] by depositing a 100- to 300-nm thick poly-M(*o*-NH_2)TPP film on a Pt minidisk followed by evaporative coating of the polymer with a thin (300 to 350 Å), porous Au film (Key Model KV-301). The Au deposition was carried out at pressures of 1 to 5 × 10^{-5} torr in intervals (50 to 100 Å each), with rates increasing from 0.5 to 1 Å/s as deposition proceeded. Each electrode assembly contained 12 Pt minidisks so that by coating six with polymer and leaving six naked (for connection to Au), six sandwiches could be prepared simultaneously. The individual sandwiches were isolated from one another following Au deposition by etching circles around pairs of Pt minidisks with a sharp wooden scribe. Sandwich electrode voltammetry (bipotentiostatic) was carried out by holding E_{Au} vs. SSCE at a fixed potential and slowly scanning E_{Pt} vs. SSCE (≤10 mV/s). The potential chosen for E_{Au} depends on the particular metalloporphyrin reaction under study; for example, E_{Au} for the Co(II)/Co(I) couple in Pt/poly-Co(*o*-NH_2)TPP/Au sandwiches was maintained at 0.0 V vs. SSCE while E_{Pt} was scanned from 0.0 to −1.3 V vs. SSCE and back. Two-electrode, solid-state voltammetry with vapor-bathed sandwich electrodes was carried out in a Vacuum Atmospheres glovebox.

Results and Discussion

Redox Couples of Pt/Poly-M(*o*-NH_2)TPP Films. For the electron self-exchange rate measurements to be meaningful, it is necessary to first establish the essential details of the redox chemistry of the polymeric metalloporphyrin sites. Cyclic voltammetry showed that, in general, their redox chemistry paralleled

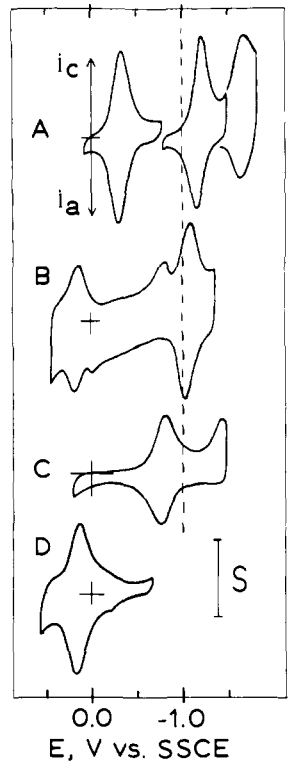

Figure 1. Cyclic voltammetric scans at 50 mV/s of different Pt/poly-Fe(*o*-NH_2)TPPX films: (A) in 0.2 M Et_4NCl/CH_3CN, Γ_T = 4.9 × 10^{-9} mol/cm^2, S = 120 μA/cm^2; (B) in 0.1 M Et_4NClO_4/CH_3CN in a drybox, Γ_T = 1.3 × 10^{-9} mol/cm^2, S = 100 μA/cm^2; (C) in incompletely deaerated 0.1 M Et_4NClO_4/CH_3CN, Γ_T = 7.2 × 10^{-9} mol/cm^2, S = 240 μA/cm^2; (D) in 0.1 M Et_4NClO_4/CH_3CN with 1 M pyridine, Γ_T = 3.2 × 10^{-9} mol/cm^2, S = 100 μA/cm^2.

that of the corresponding dissolved metalloporphyrins, including the effects of added axial ligands. A typical cyclic voltammogram of Pt/poly-Fe(*o*-NH_2)TPPCl in deaerated 0.2 M Et_4NCl/CH_3CN (Figure 1A) exhibits three prominent voltammetric waves with formal potentials ($E°'$, average of cathodic and anodic peak potentials) near those (Table I) of dissolved, monomeric Fe(*o*-NH_2)TPPCl in the same medium. These waves correspond to the three previously assigned[19,20] electrode reactions for nonaqueous reductions of substituted iron tetraphenylporphyrins:

$$[PFe^{III}]^+ + e^- \rightleftarrows [PFe^{II}]^0 \quad (1)$$

$$[PFe^{II}]^0 + e^- \rightleftarrows [PFe^{I}]^- \quad (2)$$

$$[PFe^{I}]^- + e^- \rightleftarrows [P^{\cdot-}Fe^{I}]^{2-} \quad (3)$$

where P represents the tetraphenylporphyrin dianion, and in noncoordinating solvents Fe(III) in eq 1 would be[3] five-coordinate Fe^{III}TPPCl. (CH_3CN is regarded as noncoordinating in the present study; the visible spectra in CH_2Cl_2 and CH_3CN of Fe^{III}(*o*-NH_2)TPPCl are virtually identical.)

Cyclic voltammetry of Pt/poly-Fe(*o*-NH_2)TPPCl films in 0.1 M Et_4NClO_4/CH_3CN (Figure 1B, obtained in a drybox and after several potential cycles) exhibits the Fe(II/I) reaction at a potential ($E°'_{pol}$ = −1.05 V vs. SSCE) quite close to that for Fe(*o*-NH_2)-TPPCl monomer in solution ($E°'_{soln}$ = −1.08 V vs. SSCE). The Fe(III/II) reaction for this film occurs, in contrast, at a potential 0.44 V more positive than the monomer (Table I). This difference reflects replacement in the polymer of the Cl^- axial ligand by ClO_4^-; the $Fe^{III/II}TPP(ClO_4)$ couple in butyronitrile has been reported[19] to be 0.40 V more positive than the $Fe^{III/II}$TPPCl couple. Replacement of the ordinarily stronger Cl^- ligand by ClO_4^- in the polymer is possible because Fe^{II}TPP binds Cl^- much less strongly

(17) The high electrolyte concentration promoted dissolution of the complex, possibly by a dimerization[9b] process.

(18) Potential scan rates from 20 to 100 mV/s with Γ_T up to 2 × 10^{-8} mol/cm^2 gave peak potential separations ΔE_p = 20 to 30 mV for Cu and Ni porphyrin polymers and ΔE_p = 30 to 70 mV for Fe and Co porphyrin polymers. ΔE_p values were larger for thicker films and at faster potential scan rates.

(19) Kadish, K. M. In *Iron Porphyrins*, Part II; Lever, A. B. P., Gray, H. B., Eds.; Addison-Wesley: Reading, MA, 1983; Chapter 4.

(20) Davis, D. G. In *The Porphyrins*; Dolphin, D., Ed.; Academic Press: New York, 1978; Vol. V, Chapter 4.

than does $[Fe^{III}TPP]^+$, so that Cl^- dissociation[21,22] occurs when a Pt/poly-$Fe^{III}(o\text{-}NH_2)$TPPCl film is reduced:

$$Pt/poly\text{-}Fe^{III}(o\text{-}NH_2)TPPCl \xrightarrow{e^-} Pt/poly\text{-}[Fe^{II}(o\text{-}NH_2)TPPCl]^- \rightleftarrows Pt/poly\text{-}Fe^{II}(o\text{-}NH_2)TPP + Cl^- \quad (4)$$

The dissociated Cl^- is driven out of the reduced film by diffusion as well as by the requirement for electroneutrality and after several potential scans is lost into the bulk solution and replaced by ClO_4^- when the polymer is reoxidized. Note that it is not possible to electrochemically prepare ClO_4^- or other weakly coordinated metal porphyrin complexes from *dissolved*, monomeric Fe(o-NH_2)-TPPCl in an analogous in situ manner. In solution, both Fe^{II}-(o-NH_2)TPP and Cl^- reduction products coexist in the diffusion layer, and Cl^- is freely available to recoordinate to $[Fe^{III}(o\text{-}NH_2)TPP]^+$ upon oxid .ion.

We were also able to detect formation of what is apparently a Pt/poly-$[Fe^{III}(o\text{-}NH_2)TPP]_2O$ μ-oxo-bridged dir r in the cyclic voltammetry of Pt/poly-$Fe^{III}(o\text{-}NH_2)$TPPCl films in poorly deaerated 0.1 M Et_4NClO_4/CH_3CN solutions (Figure 1C). The formal potential ($E^{\circ\prime}$ = −0.78 V vs. SSCE) of the wave which develops after several potential scans is quite different from those of the three electrode reactions of Fe(o-NH_2)TPPCl (Table I). μ-Oxo dimers are known[15a] to form by reactions between sterically unhindered Fe(II) porphyrins and dioxygen, and solutions of $[Fe^{III}TPP]_2O$ in DMF[15b] and in pyridine[15c] are electrochemically reduced to the Fe(III)Fe(II) mixed-valent complex at −0.93 and −1.03 V vs. SCE, respectively. While our observed wave is less negative than these (but is in CH_3CN solvent), and we have no spectral data, assignment of the voltammetry of Figure 1C to reduction of Pt/poly-$[Fe^{III}(o\text{-}NH_2)TPP]_2O$ is supported by the observation that the film voltammetry in 0.2 M Et_4NCl/CH_3CN reverts to that of Figure 1A after soaking the film for ca. 1 min in 0.06% $HClO_4$ in CH_3CN. Acid hydrolysis (with HCl) is a known method for converting $[FeTPP]_2O$ to FeTPPCl.

In 0.1 M Et_4NClO_4/CH_3CN containing 1 M pyridine, films of poly-Fe(o-NH_2)TPPCl exhibit, after a few cyclical scans, voltammetry as in Figure 1D. In the pyr line medium, after Cl^- has been released from the film by elec ogenerating Fe(II), it is expected[19] that both the Fe(III) and Fe(II) porphyrin states will be coordinated by two molecules of pyridine. The considerably more positive polymer $E^{\circ\prime}$ (0.15 V vs. SSCE, Table I) shows that *relative* to the effects of Cl^- coordination, pyridine coordination stabilizes the Fe(II) state more than the Fe(III) state.

In cobalt metalated films, the Co(III/II) electrode reactions are very slow, and satisfactory cyclic or sandwich electrode voltammetry could not be obtained. The Co(II/I) cyclic voltammetry[20] in Pt/poly-Co(o-NH_2)TPP films is, on the other hand, well behaved, and in 0.1 M Et_4NClO_4/CH_3CN $E^{\circ\prime}$ = −0.86 V vs. SSCE (Figure 2A) and with added 1 M pyridine $E^{\circ\prime}_{pol}$ = −1.06 V vs. SSCE (Table I). The difference in potential occurs because[6,23] copper(II) tetraphenylporphyrin normally binds a single axial pyridine ligand from noncoordinating solvents, while the Co(I) state exhibits no affinity for pyridine. This change in axial coordination between Co(II) and Co(I) states and the consequent $E^{\circ\prime}$ variation with log [py] are important features of the electron transport as will be seen in a later section.

Reductions of Ni(II) and Cu(II) porphyrins ordinarily[20] yield metal(II) porphyrin (radical anion) states. We have reported[9a] the cyclic voltammetry of Pt/poly-Ni(o-NH_2)TPP films in 0.1 M Et_4NClO_4/CH_3CN, and Pt/poly-Cu(o-NH_2)TPP films behave nearly identically (Table I).

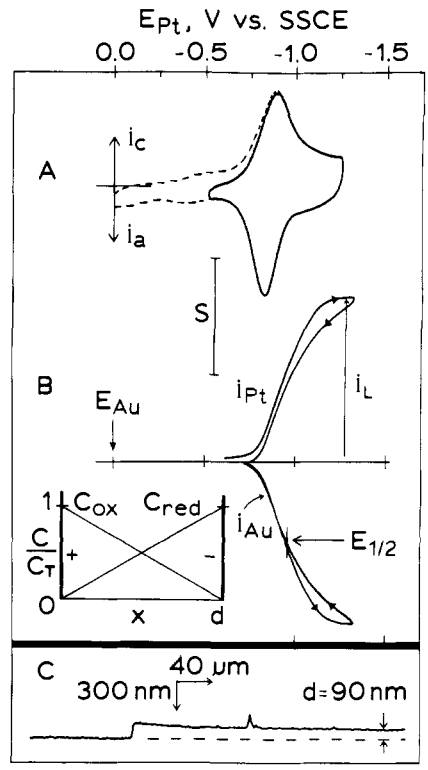

Figure 2. Voltammograms in 0.1 M Et_4NClO_4/CH_3CN, $\Gamma_T = 1.2 \times 10^{-8}$ mol/cm^2: (A) cyclic voltammetry of Pt/poly-Co(o-NH_2)TPP at 20 mV/s, S = 200 μA/cm^2; (B) four-electrode voltammetry of Pt/poly-Co(o-NH_4)TPP/Au sandwich electrode with E_{Au} = 0.0 V, E_{Pt} at 5 mV/s, S = 400 μA/cm^2; (C) surface profilometry at the edge of a poly-Co(o-NH_2)TPP film on SnO_2/glass, $\Gamma_T = 7.6 \times 10^{-9}$ mol/cm^2.

Electron-Transport (Electron-Hopping) Rates in Solution-Bathed Pt/Poly-M(o-NH_2)TPP/Au Sandwiches. Applying electrode potentials as described in the Experimental Section gives the steady-state sandwich voltammogram in Figure 2B for a Pt/poly-Co(o-NH_2)TPP/Au sandwich containing about 120 porphyrin monolayers (ca. 0.14 μm) and immersed in deaerated 0.1 M Et_4NClO_4/CH_3CN. The concentration–distance inset of Figure 2B explains that the limiting current of the voltammogram corresponds to the condition that all of the porphyrin sites have been converted to Co(I) at the (negative) Pt/porphyrin interface, while all of those at the (positive) Au/porphyrin interface are Co(II). Linear concentration gradients of Co(II) and Co(I) sites exist across the polymer film in between, and these gradients of concentration drive electron self-exchange reactions between neighbor Co(II) and Co(I) sites to yield a steady, net current flow. As shown previously,[25] the corresponding electron-hopping rate is stated in terms of the electron diffusion coefficient D_e via Fick's first law:

$$i_L = nFAD_eC_T/d = nFAD_eC_T^2/\Gamma_T \quad (5)$$

where n is mol of electrons/equiv, F the Faraday, A the Pt minidisk area, C_T the volume concentration of porphyrin redox sites, and d the porphyrin film thickness. The product $D_e^{1/2}C_T = 8.1 \times 10^{-9}$ mol/cm^2·s$^{1/2}$ is obtained from the limiting current in Figure 2B with no assumptions. C_T was evaluated as 0.85 (±0.03) M electroactive porphyrin sites in dry polymer films of known coverage (Γ_T) on SnO_2-coated glass slides using surface profilometry thickness measurements (Figure 2C). Neglecting polymer swelling effects, this C_T gives $D_e = 9.1 \times 10^{-11}$ cm^2/s as a measure of the rate of electron self-exchange between Co(II) and Co(I) sites in

(21) Kadish, K. M.; Rhodes, R. K. *Inorg. Chem.* **1983**, *22*, 1090.

(22) The weakly coordinated $[Fe^{II}(o\text{-}NH_2)TPPCl]^-$ species can (eq 4) exist[21] in media containing excess Cl^-, as can be seen by comparison of the Fe(II/I) potentials observed for both monomer and polymer in 0.1 M Et_4NClO_4/CH_3CN and 0.2 M Et_4NCl/CH_3CN (Table I). Stability constants K of 800 and 540 M^{-1} for the Fe(II)–chloro complex for monomer and polymer (assuming unity partition coefficient of Cl^-), respectively, can be estimated from the 0.12–0.13 V potential shift.

(23) (a) Lin, X. Q.; Boisselier-Cocolios, B.; Kadish, K. M. *Inorg. Chem.* **1986**, *25*, 3242. (b) Rocklin, R. D.; Murray, R. W. *J. Electrochem. Soc.* **1980**, *127*, 1979.

(24) The currents on the negative- and positive-going potential scans show a slight and inconsequential hysteresis due to the finite rate of potential scan of E_{Pt}.

(25) (a) Murray, R. W. In *Electroanalytical Chemistry*; Bard, A. J., Ed.; Marcel Dekker, New York, 1984; Vol. 13, p 191. (b) Murray, R. W. *Annu. Rev. Mater. Sci.* **1984**, *14*, 145.

Table II. Rate Constants for Electron Diffusion and Heterogeneous Electron Transfer for Several Metalloporphyrins

reaction[a]	medium[b]	$D_e^{1/2}C^c$ (mol/cm^2·s$^{1/2}$)	D_e^d (cm^2/s)	$k_{ex}^{app\,d,m}$ (M^{-1} s^{-1})	k^0 (lit.) (cm s)	medium[f]
$PFe^{III/II}$					8.4×10^{-4}	Bu_4NClO_4/DMF[g,h]
$PFe^{III/II}$	Et_4NCl/CH_3CN	4.8×10^{-9}	3.3×10^{-11}	2.5×10^3	3.1×10^{-3}	$Bu_4NClO_4/PrCN$[h,i]
$PFe^{II/I}$	Et_4NCl/CH_3CN	5.0×10^{-9}	3.5×10^{-11}	2.6×10^3	7.4×10^{-3}	$Bu_4NClO_4/PrCN$[h,i]
$(P^{0/\cdot-})Fe^I$	Et_4NCl/CH_3CN	2×10^{-8}	5×10^{-10}	3.8×10^4	1.0×10^{-2}	$Bu_4NClO_4/PrCN$[h,i]
$PFe^{III/II}$	Et_4NClO_4/1 M py/CH_3CN	5.5×10^{-8}	4.2×10^{-9}	3.2×10^5	5.2×10^{-2}	Bu_4NClO_4/2 M py/DMF[g]
$(1\text{-MeIm})_2PFe^{III/II}$					(8.1×10^7 M^{-1} s^{-1})[j]	CD_2Cl_2
$PFe^{III/II}$	py/CH_3CN vapor[e]	3.3×10^{-8}	1.6×10^{-9}	1.2×10^5		
$PCo^{II/I}$	Et_4NClO_4/CH_3CN	8.0×10^{-9}	9.0×10^{-11}	6.8×10^3	7.4×10^{-3}	$Bu_4NClO_4/PrCN$[k]
$PCo^{II/I}$	Et_4NClO_4/1 M py/CH_3CN	3.1×10^{-9}	1.4×10^{-11}	1.1×10^3	4.5×10^{-3}	Bu_4NClO_4/1.24 M py/PrCN[k]
$(P^{0/\cdot-})Ni^{II}$	Et_4NClO_4/CH_3CN	8.8×10^{-8}	1.1×10^{-8}	8.3×10^5	3.7×10^{-2}	Bu_4NClO_4/CH_2Cl_2[l]
$(P^{0/\cdot-})Cu^{II}$	Et_4NClO_4/CH_3CN	1.6×10^{-7}	3.7×10^{-8}	2.8×10^6		

[a] P represents the dianion of (*o*-NH_2)TPP in electropolymerized films for electron diffusion rates on the left of the table. P represents the dianion of tetraphenylporphyrin, unless otherwise noted, for the heterogeneous electron-transfer rates (k^0) given on the right-hand side of the table. [b] [Et_4NCl] = 0.2 M; [Et_4NClO_4] = 0.1 M. [c] Relative standard deviations are 5 to 20%. [d] Relative standard deviations are 10 to 40%. [e] Vapor above 1 M pyridine/CH_3CN. [f] [Bu_4NClO_4] = 0.1 M. [g] Reference 5; DMF is *N*,*N*-dimethylformamide; P is protoporphyrin IX. [h] Cl^- is available as axial ligand during electrochemistry because the iron porphyrins are used as chlorides. [i] Reference 3; PrCN is *n*-butyronitrile. [j] This k_{ex}^{homo} was determined at −21 °C by NMR (ref 7a); 1-MeIm is 1-methylimidazole. [k] Reference 6; PrCN is *n*-butyronitrile. [l] Reference 4. [m] Calculated from eq 6 using ΔX = 1.25 nm which is average site–site separation based on 0.85 M site concentration.

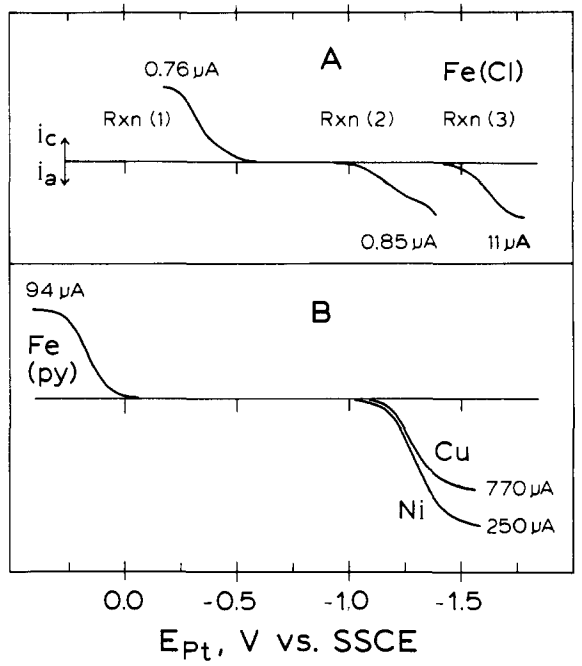

Figure 3. Curves of sandwich electrode currents measured at gold (i_{Au}) vs. E_{Pt} of Pt/poly-M(*o*-NH_2)TPP/Au sandwich electrodes in various media. The usual current scales are replaced with numbers by curves showing values of i_L (μA) normalized to $\Gamma_T = 1.0 \times 10^{-8}$ mol/cm^2, electrode area = 0.0032 cm^2. Panel A: Pt/poly-Fe(*o*-NH_2)TPPCl/Au sandwiches in 0.2 M Et_4NCl/CH_3CN using potential ranges corresponding to Fe(III/II), Fe(II/I), and $P^{0/-}Fe^I$, eq 1–3, respectively; E_{Pt} scanned at 2.5 mV/s; E_{Au} = −0.7 V for eq 1 and 2; E_{Au} = −1.4 V for eq 3. Panel B: Pt/poly-Fe(*o*-NH_2)TPP(py)$_2$/Au sandwich with 1 M pyridine present, Fe(III/II) reaction; Pt/poly-Cu(*o*-NH_2)TPP/Au and Pt/poly-Ni(*o*-NH_2)TPP/Au sandwiches, $P^{0/-}M^{II}$ reactions; all in 0.1 M Et_4NClO_4/CH_3CN with E_{Pt} scanned at 10 mV/s; E_{Au} = −0.15 V.

the Pt/poly-Co(*o*-NH_2)TPP/Au sandwich.

Analogous sandwich electrode voltammetry experiments for other poly-M(*o*-NH_2)TPP films are illustrated in Figure 3. Whether the gold electrode currents shown are cathodic or anodic varies simply according to whether E_{Au} was chosen to be more negative or positive than the porphyrin formal potential. The values of limiting currents shown in the figure are those which would be obtained for a 1×10^{-8} mol/cm^2 film of the particular porphyrin, to emphasize that the limiting currents strongly depend on the metalloporphyrin polymer. The measured electron diffusion coefficients are given in Table II.

The values of D_e shown in Table II represent the experimental goal of this work, and it was therefore significant that they show a wide range of variation with porphyrin metal, oxidation state couple, and axial ligand. In measuring the rate of electron hopping in the polymeric porphyrins, we must recall[25] that there are several factors that can constitute the main barrier for the hopping event. These factors include (i) motions of charge-compensating counterions, (ii) polymer lattice fluidity, and (iii) the so-called "intrinsic" energy barrier. In the last case, we refer to the situation in which electron transfers between the oxidized and reduced polymeric porphyrin sites are so unimpeded by ion or polymer lattice motions, and so unchanged by the polymeric solvation environment, that the electron-transfer barrier is a good approximation of that which would be observed for reactions between the corresponding monomers in solutions. Clearly, this situation would be a valuable result in the chemical sense of general applicability of the present experiment to metalloporphyrinic electron-transfer kinetics.

To test the relationship of electron diffusion coefficients obtained in polymer films to electron-transfer kinetics of porphyrin monomers in solution, we need either (a) a comparison of counterion diffusion coefficients or polymer chain self-diffusion coefficients to D_e, or (b) a comparison of D_e constants obtained over a range of polymeric porphyrin redox couples (as in Table II) to kinetic data that describe monomeric porphyrin self-exchange rates in solution. We have no data in hand for ion or polymer chain self-diffusion coefficients in these polymers. However, it is relevant to note that D_e varies by a factor of 10^3 (Table II), but the porphyrinic polymers are all derived from the *same* o-aminophenyl oxidative coupling reaction, and similar (ClO_4^- and Cl^-) counterions are used. The magnitude of the D_e variation in comparison to these constant chemical features is strong evidence that counterion and polymer lattice mobilities do not dominate the electron-hopping barriers for the polymeric porphyrins.

There are inadequate homogeneous solution electron self-exchange data[7a] to compare to the D_e results, but a reasonable range of data exists[2-6] for the heterogeneous electron-transfer rates (k^0) of tetraphenylporphyrin *monomers* at electrode surfaces (see Table II). For comparison to these data, we first invoke the relation between D_e and the more familiar electron self-exchange rate constant as formulated[14,26] by Laviron and by Saveant:

$$D_e = 10^3 k_{ex}^{app} C_T (\Delta x)^2 \qquad (6)$$

(26) (a) In a previous work,[11] conversion of D_e into k_{ex}^{app} was done using the Smoluchowski equation:[26b] $k_{ex}^{app} = (4 \times 10^{-3})\pi N(4rD_e)$, where N is Avogadro's number and r is the reactant radius (equal to $0.5\Delta x$ for an undiluted, fixed-site redox polymer). Approximating C_T in eq 6 as $[(\Delta x)^3 N]^{-1}$ gives $k_{ex}^{app} = 10^{-3}(\Delta x)ND_e$ which is functionally identical with the Smoluchowski equation and differs only by a numerical factor of 4π upon including the previously overlooked[11] symmetry factor[26b] of 0.5 in the Smoluchowski equation. For localized-state redox polymers with *diluted* sites, the *average* site separation (Δx) used in eq 6 will be larger than the contact distance ($2r$) used in the Smoluchowski equation (but seems unrelated to the factor of 4π difference still under scrutiny). (b) Hammes, G. G. *Principles of Chemical Kinetics*; Academic Press: New York, 1978; pp 64 and 34.

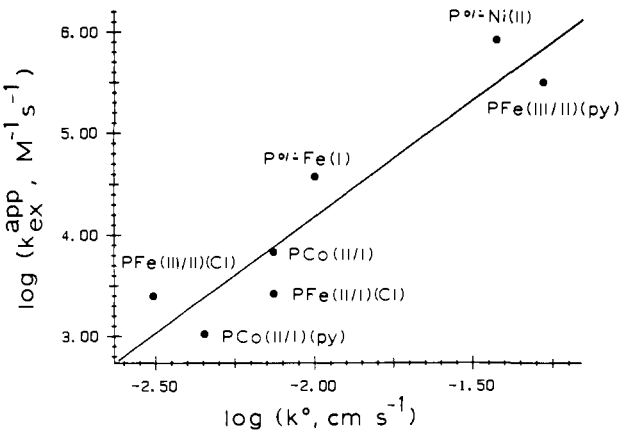

Figure 4. Plot of apparent electron self-exchange rate constants k_{ex}^{app}, derived from polymer D_e values in Table II using eq 6, vs. heterogeneous electron-transfer rate constants k^0 in Table II for monomers.

where k_{ex}^{app} is the self-exchange rate constant in the polymer in M^{-1} s^{-1}, C_T is the volume concentration of redox sites in mol/cm^3, and Δx is the average distance between redox sites in the film in cm. Note that in this theory, Δx may actually be greater than the reactant separation in the transition state, but since we are dealing with a polymer containing essentially undiluted redox sites this should have only a small effect. Values of k_{ex}^{app} calculated on the basis of eq 6 are given in Table II and compared to the literature heterogeneous electron-transfer kinetic data in Figure 4.

Although there is some scatter, the comparison of Figure 4 clearly shows that the D_e-derived polymeric electron self-exchange kinetic data parallel the results of monomer solution experiments. The comparison includes the following chemically expected points: (a) the ligand-centered reactions, $(P^{0/\bullet-})$Ni(II) and $(P^{0/\bullet-})$Cu(II) (see Table II), exhibit the fastest electron-transfer rates, and the ligand-centered reaction of $(P^{0/\bullet-})Fe^{I}$ is the fastest of the Fe couples in the chloride medium; (b) the kinetics of Co metal-centered reactions are slowest when a strongly binding ligand (e.g., py) is dissociated as part of the self-exchange event; and (c) the Fe(III/II) metal-centered reaction is quite fast for ligands (e.g., py) that give low-spin six-coordinate complexes undergoing no axial changes upon electron transfer.[27] We believe that this comparison supports our proposal that polymeric porphyrin electron diffusion coefficient measurements can be used to probe the electron self-exchange kinetics of other, less familiar porphyrin systems that can be incorporated into polymeric form.

There is another important aspect of Figure 4. While the data scatter requires caution, the data appear to fit the slope of 2 anticipated if the heterogeneous electron-transfer rate constants (k^0) of Table II can be linked to the homogeneous (k_{ex}^{homo}) electron-transfer rate constants by the familiar relation[28]

$$k_{ex}^{homo} = [Z_{homo}/Z_{het}^2](k^0)^2 \qquad (7)$$

where Z_{homo} and Z_{het} are the homogeneous (10^{11} M^{-1} s^{-1}) and heterogeneous (10^4 cm s^{-1}) collision frequencies, respectively. The satisfactory quantitative comparison ends there, however, because the values of k_{ex}^{homo} calculated from eq 7 are consistently smaller by a factor of between 10^4 and 10^5 than k_{ex}^{app} values derived from eq 6. Application of eq 7 has often led to large differences between rate constants, and various types of corrections have been discussed by Weaver et al.[29]

Effect of Pyridine Concentrations on the Electron Diffusion Rate in Pt/Poly-Co$^{II/I}$(o-NH$_2$)TPP/Au Sandwiches. The voltammetric half-wave potential $E_{1/2}$ and the limiting current i_L for electron transport by the Co(II/I) reaction vary systematically with the pyridine concentration, [py], added to the bathing solution (Figure

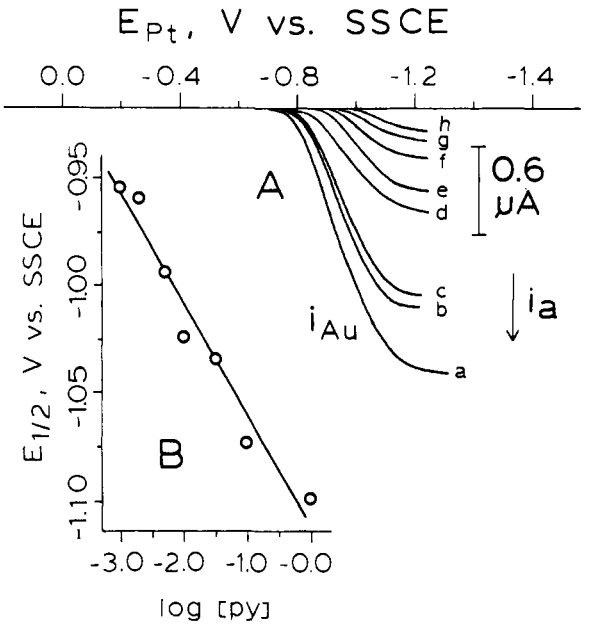

Figure 5. (A) Forward-going i_{Au} vs. E_{Pt} curves on the same Pt/poly-Co(o-NH$_2$)TPP/Au sandwich electrode in 0.1 M Et_4NClO_4/CH_3CN with various concentrations of pyridine; $\Gamma_T = 1.2 \times 10^{-8}$ mol/cm^2; electrode area = 0.0032 cm^2; $E_{Au} = 0.0$ V; E_{Pt} at 5 mV/s; curves a–h: [py] = 0.0, 1×10^{-3}, 2×10^{-3}, 5×10^{-3}, 1×10^{-2}, 3.16×10^{-2}, 1×10^{-1}, and 1 M, respectively. (B) Plot of $E_{1/2}$ vs. log [py] for curves b–h in (A); least-squares line has slope = 52 (±5) mV, correlation coefficient = 0.978.

Scheme I

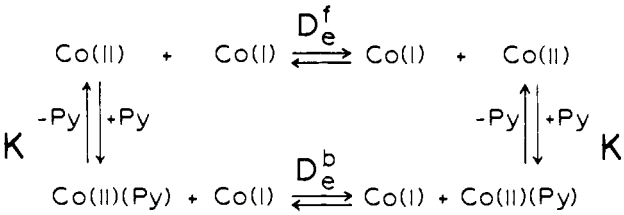

5). These experimental features were exploited for a more detailed analysis of this process. In noncoordinating solvents,[6,23] including CH_3CN,[30] Co(II) porphyrins are known to bind a single axial pyridine ligand, while Co(I) is uncomplexed by pyridine. If the same chemistry applies to the polymeric porphyrin, the variation in $E_{1/2}$ of the poly-Co$^{II/I}$(o-NH$_2$)TPP voltammetric wave with [py] is accordingly[30]

$$(E_{1/2})_b = E(_{1/2})_f - 0.059 \log KP[py] \qquad (8)$$

where the subscripts b and f denote potentials of the bound (coordinated) and free Co(II) species, respectively; K is the stability constant of the Co(II)–pyridine complex; and P is the partition coefficient of pyridine into the polymer ($P = [py]_{film}/[py]$). Figure 5B shows half-wave potential data plotted according to eq 8; the linear plot has a slope of 52 mV/decade which is close to the 59 mV/decade expected for loss of one pyridine axial ligand upon electron transfer. The intercept of Figure 5B gives log KP = 2.7 (KP = 500 M^{-1}) which, assuming $P \sim 1$, is within the range of log K values (2.4 to 2.9) that have been reported for Co^{II}TPP(py) in several solvents.[31]

To explain the interesting, reversible[32] variation in i_L with [py], Figure 5A, we propose Scheme I, which involves parallel pathways for electron transport. The upper pathway represents transport by electron self-exchanges between Co(II)–acetonitrile and Co(I)

(27) Kadish, K. M.; Su, C. H. *J. Am. Chem. Soc.* **1983**, *105*, 177.
(28) (a) Marcus, R. A. *J. Phys. Chem.* **1963**, *67*, 853. (b) Marcus, R. A. *Ibid.* **1965**, *43*, 679.
(29) (a) Weaver, M. J.; Hupp, J. T. *ACS Symp. Ser.* **1982**, *No. 198*, 181. (b) Weaver, M. J. *J. Phys. Chem.* **1980**, *84*, 568. (c) Hupp, J. T.; Weaver, M. J. *Inorg. Chem.* **1983**, *22*, 2557.
(30) Jester, C. P.; Rocklin, R. D.; Murray, R. W. *J. Electrochem. Soc.* **1980**, *127*, 1979.
(31) (a) Yamamoto, K. *Inorg. Chim. Acta* **1986**, *113*, 181. (b) Kadish, K. M.; Bottomly, L. A.; Beroiz, D. *Inorg. Chem.* **1978**, *17*, 1124.
(32) The higher currents through the polymer can be restored by soaking the sandwich in pyridine-free 0.1 M Et_4NClO_4/CH_3CN followed by electrochemical reduction to the Co(I) state to release any remaining pyridine.

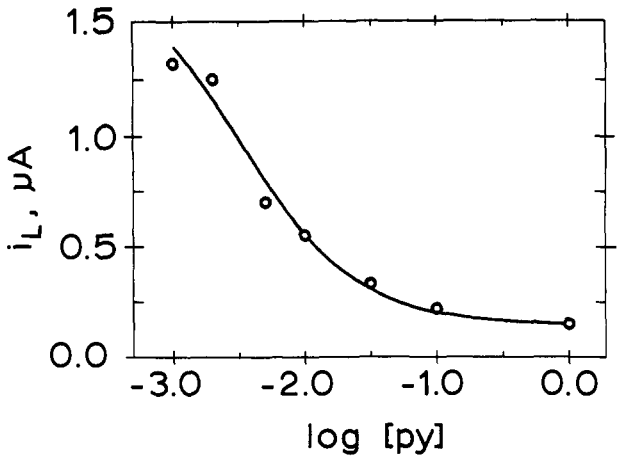

Figure 6. (O) Plot of experimental i_L vs. log [py] for curves b–h in Figure 5. (—) Plot of eq 10 using $KP = 300\ M^{-1}$, $D_e^f = 9.1 \times 10^{-11}$ cm^2/s, $D_e^b = 7.7 \times 10^{-12}$ cm^2/s, $\Gamma_T = 1.2 \times 10^{-8}$ mol/cm^2, and electrode area = 0.0032 cm^2.

porphyrin states, characterized by the $D_e^f = 9 \times 10^{-11}$ cm^2/s measured in the absence of pyridine (Table II). The lower pathway represents electron transport by self-exchanges between Co(II)–pyridine and Co(I) porphyrin states, characterized by the $D_e^b = 1.4 \times 10^{-11}$ cm^2/s measured at such high [py] (1 M) that all of the Co(II) is axially coordinated.[33] In the intermediate pyridine concentration range, the Co(II) state is proposed to equilibrate according to K, and the net i_L is simply the sum of the currents for the two pathways. This yields

$$i_L = nFA(D_e^f C_f^2/\Gamma_f + D_e^b C_b^2/\Gamma_b) \qquad (9)$$

which can be simplified using $KP = C_b/C_f[py]$ and $C_T = C_b + C_f = 0.85$ M to yield

$$i_L = \frac{nFAC_T^2(D_e^f + D_e^b KP[py])}{\Gamma_T(1 + KP[py])} \qquad (10)$$

Figure 6 shows that using KP as a fitting parameter in eq 10 to predict i_L as a function of [py] produces (—) a very good match to experimental data (O) for $KP = 300\ M^{-1}$ (log $KP = 2.48$). This result was typical of several trials and (assuming $P = 1$) agrees reasonably with both the literature[31] values of log K (2.4 to 2.9) and the $KP = 500\ M^{-1}$ obtained from Figure 4B.

These results both establish the validity of the parallel electron transport scheme and the similarity of the chemical properties of the polymeric cobalt porphyrin to solution behavior. The latter property is further consistent with the interpretation of D_e values in Table II and Figure 4.

Voltammetry Using Vapor-Bathed Pt/Poly-Fe(o-NH$_2$)TPP-(py)$_2$/Au Sandwiches. Given a polymer film sandwich electrode that contains both oxidizable and reducible sites, and also a resident population of mobile charge-compensating counterions, electrochemical reactions and electron transport can be observed when the sandwich electrode is bathed only in solvent vapors[12] (rather than being exposed to an electrolyte solution as was the case in all the above experiments). We report some preliminary experiments of this nature for Pt/poly-Fe(o-NH$_2$)TPPCl/Au sandwich electrodes. The films were first cycled to expel Cl^- and then electrochemically charged to the 1:1 Fe(III/II) mixed-valent state in a drybox by applying the couple's formal potential as determined from cyclic voltammetry (arrow in Figure 7A) in 0.1 M Et_4NClO_4/1 M pyridine/CH_3CN. The mixed-valent polymer sandwiches were then removed from the solution, rinsed with electrolyte-free 1 M pyridine/CH_3CN, and allowed to dry in the glovebox atmosphere.

Voltammetry corresponding to electron transport via the Fe(III/II) self-exchange reaction results when the potential difference between the Pt and Au electrodes is scanned. This voltammetry proved to be very sensitive to the gaseous bathing environment into which the sandwich electrode is placed, and reflects how the self-exchange kinetics change with internal solvation of the polymer. Figure 7B shows the voltammogram obtained when a Fe(III/II) sandwich is exposed to the vapor of a 1 M pyridine solution in CH_3CN. At a sufficiently large ΔE (±0.3 V), the Fe(III) and Fe(II) concentration gradients are completely polarized (as in Figure 2B). The electron diffusion coefficient $D_e = 1.6 \times 10^{-9}$ cm^2/s (Table II) for the Fe(III/II) couple under these nonliquid circumstances, obtained by application of eq 5, is about 40% as large as that obtained when the electrodes were bathed in the 1 M pyridine/CH_3CN liquid (4.2×10^{-9} cm^2/s). That is, electron transport is *slowed* in the vapor-bathed case.

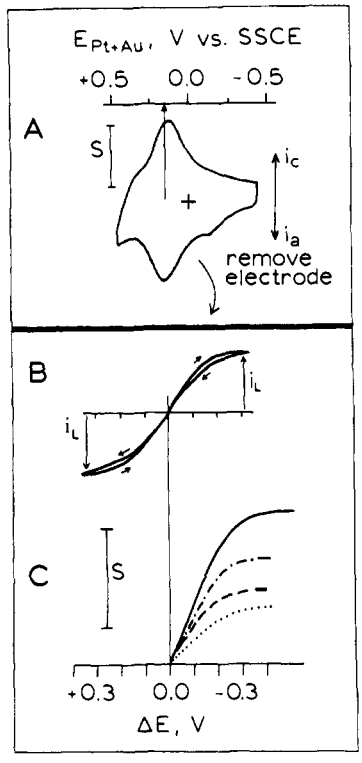

Figure 7. Voltammetry of Pt/poly-Fe(o-NH$_2$)TPP(py)$_2$/Au sandwich electrodes in various media in a drybox; (A) and (B) are of the same electrode with $\Gamma_T = 2.1 \times 10^{-8}$ mol/cm^2. (A) Cyclic voltammetry in 0.1 M Et_4NClO_4/1 M pyridine/CH_3CN using Pt and Au electrodes shorted together and swept at 33 mV/s; $S = 400$ μA/cm^2. Scan stopped at arrow to prepare 1:1 mixed valent film. (B) In py/CH_3CN vapor above 1 M pyridine/CH_3CN scanning ΔE between the two electrodes at 10 mV/s; $S = 10$ mA/cm^2. (C) As in (B) but in vapors of various composition; ΔE scan at 10 mV/s; $\Gamma_T = 2.3 \times 10^{-8}$ mol/cm^2; $S = 2.5$ mA/cm^2; bathing vapors, in the order of experiments: (—) above 1 M pyridine-/CH_3CN, (···) above pure pyridine, (- - -) above pure CH_3CN, (-···) again above 1 M pyridine/CH_3CN.

Figure 7C shows the result of exposing another mixed-valent sandwich electrode sequentially to the vapors of (—) 1 M pyridine/acetonitrile, pure pyridine (···), pure acetonitrile (- - -), and then 1 M pyridine/acetonitrile again (-····). Currents in the last curve are smaller than in the first, suggesting that the electrode has experienced some decay. However, the sequence of effects clearly shows that electron transport is facilitated by the *combination* of pyridine and acetonitrile. The two components of the vapor may serve different functions, perhaps CH_3CN as plasticizer and pyridine as axial ligand.

These preliminary solid-state voltammetry experiments show that it may be possible to explore porphyrin electron self-exchange kinetics over a broader range of solvation and axial coordination conditions than is possible in conventional solutions of monomers.

Acknowledgment. The authors thank K. M. Kadish for a preprint of ref 23 and Drs. A. Bettelheim and S. A. Raybuck for helpful discussions. This research was supported in part by a grant from the National Science Foundation.

(33) If $K = 300\ M^{-1}$, ≥99% of the Co(II) sites in the film are coordinated by pyridine when [py] = 1 M and $P = 1$.